Versatility of bilayer metal oxide coatings on silver nanowire networks for enhanced stability with minimal transparency loss

Sara Aghazadehchors[1,2], Viet Huong Nguyen[1], David Muñoz-Rojas[1,*], Carmen Jiménez[1], Laetitia Rapenne[1], Ngoc Duy Nguyen [2], Daniel Bellet[1,*]

[1] *Univ. Grenoble Alpes, CNRS, Grenoble INP, LMGP, F-38000 Grenoble, France*
[2] *Département de Physique, Université de Liège, CESAM/Q-MAT, SPIN, B-4000 Liège, Belgium.*
Corresponding authors: david.munoz-rojas@grenoble-inp.fr; daniel.bellet@grenoble-inp.fr

Supplementary Information:

1. AP-SALD deposition system

Our group has developed a "close-proximity" Atmospheric Pressure Spatial Atomic Layer Deposition (AP-SALD) reactor, in which the different precursors are supplied along parallel channels kept and away by adjacent inert gas-flow channels[1] as shown in figure SI-1 a. It is essential to place the substrate close enough (i.e. at a distance smaller than 200 micrometers in the present experimental conditions) to the gas injector to ensure that precursor mixing is occurring only on the substrate rather than in the gas phase (avoiding then the CVD mode). Substrate oscillates below the injection head providing the ALD cycles to yield film growth. The designed system is capable of operation in atmospheric condition with no need of a deposition chamber. More details can be found in the already published articles by our team with the papers of Munoz et al. [2], Nguyen et al.[3] and Masse de la Huerta et al.[4].

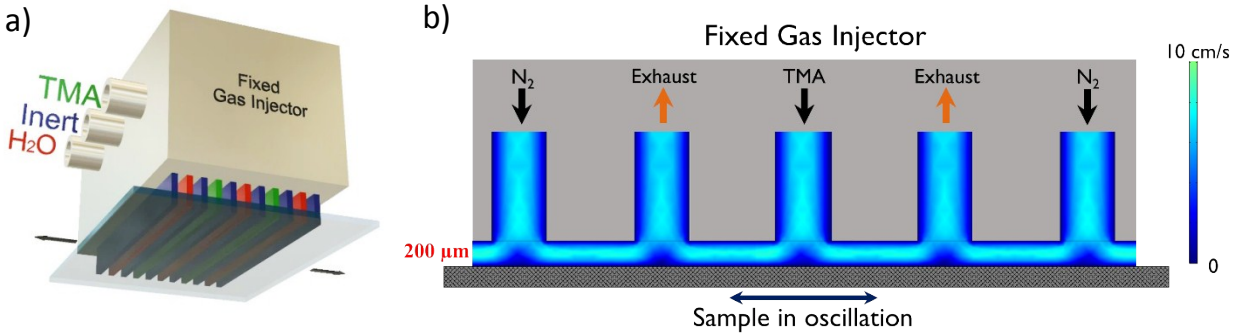

Figure SI-1: Schematic representations of a) an AP-SALD gas injector with three gas inlets of trimethylaluminum (TMA), inert gas (N_2), and H_2O, which are then continuously injected to a moving substrate, the gas exhaust channels are not shown in this figure; b) a zoom in the cross-section view of the gas injector, which shows the exhaust channels alternatively located between gas outlets (the color showing the gas velocity, computed using COMSOL Multiphysics Simulation). This schematic represents deposition of Al_2O_3, while the injector head for ZnO has the identical design, TMA is replaced by diethylzinc (DEZ).

2. EDS STEM imaging on Al_2O_3 coated AgNWs

In order to confirm the presence of Al_2O_3 coating on AgNWs, EDS measurements were performed by STEM with a JEOL 2100F FEG microscope operating at 200 kV with a 0.2 nm resolution in the scanning mode. The novel JEOL SDD Centurio detector with a large solid angle of up to 0.98 steradians was used for the EDS experiments. In order to prepare the samples for TEM imaging, the AgNW solution is directly deposited on Holey carbon coated copper grid by dip coating. After annealing of samples at 230°C for 60 minutes, TEM grids were fixed on a corning substrate using Kapton tape and SALD of Al_2O_3 coating was performed. Using this approach there was no need of specimen preparation of coated AgNWs on to the TEM grids, therefore high quality images with no damage on the NWs and coatings could be acquired. As reported by Figure SI-2 STEM EDS imaging results confirmed the presence of a significant layer of Al_2O_3 as expected.

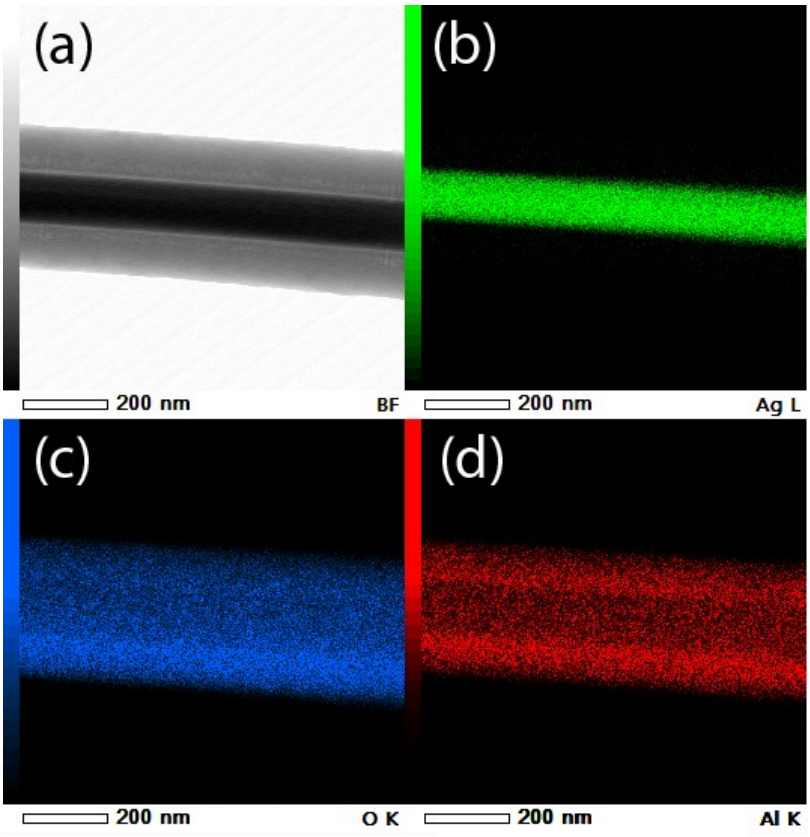

Figure SI-2. (a) Bright-field STEM image of a AgNW coated with Al_2O_3 layer (the average diameter of AgNWs being 90 nm). Corresponding EDS mapping of the (b) Ag, (c) O, (d) Al elements.

3. TEM observations of Ag atoms diffusion through ZnO coatings

To prevent instability of AgNW networks a coating with metal oxide (ZnO or Al_2O_3) is performed, this hinders Ag atomic diffusion and enhances the morphological stability of AgNWs and the stability of the associated networks when submitted to electrical or thermal stress. When a too large stress is applied AgNW electrical resistance increases. An example is reported in Figure SI-3 of a AgNW network after a thermal annealing at 400°C for 30 minutes: Bright-field STEM image and STEM EDS observations clearly reveal that Ag atoms have diffused through the 45 nm ZnO coating, resulting in the network failure.

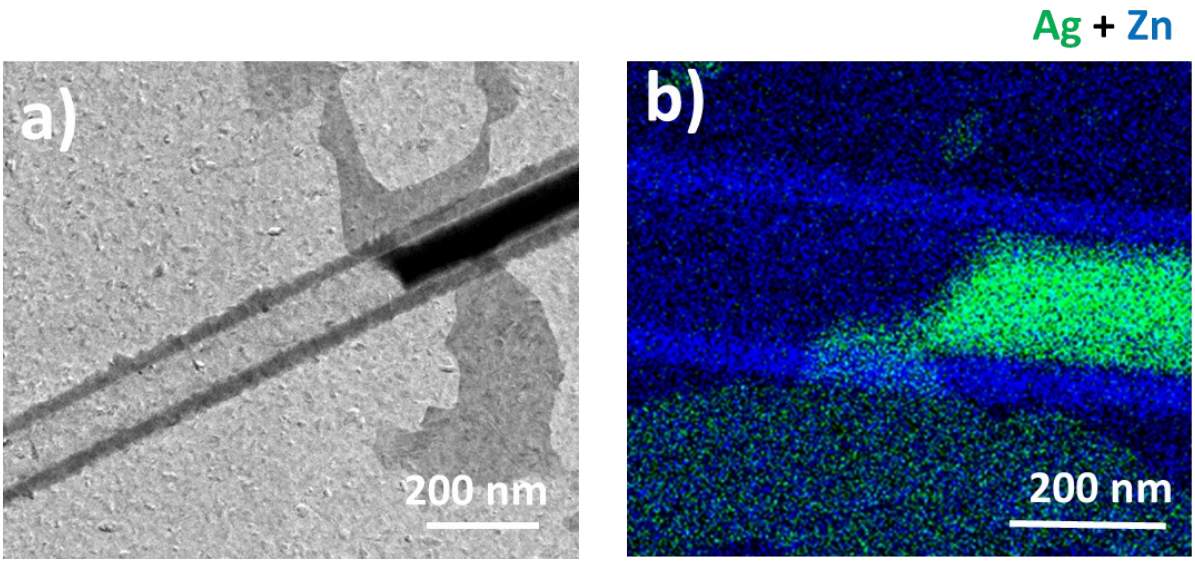

Figure SI-3. (a) Bright-field STEM image and (b) EDS STEM imaging of the thermal degradation of 45 nm ZnO coated AgNW networks after thermal stress (400 °C for 30 minutes).

4. Delamination of Al_2O_3 coated AgNWs

Delamination of multilayer thin films at elevated temperatures is a well-known phenomenon.[5] The difference in thermal expansion between different films can induce stress and initiate buckling and further forms micro cracks. The initial microcracks can elongate through the films and cause ultimate delamination of films. Examples of such process were observed on Al_2O_3 coated AgNWs on glass substrate after thermal annealing up to 400 °C (with a thermal rate of 2°C min^{-1}). SEM images clearly show delamination of coated AgNW films from glass substrate.

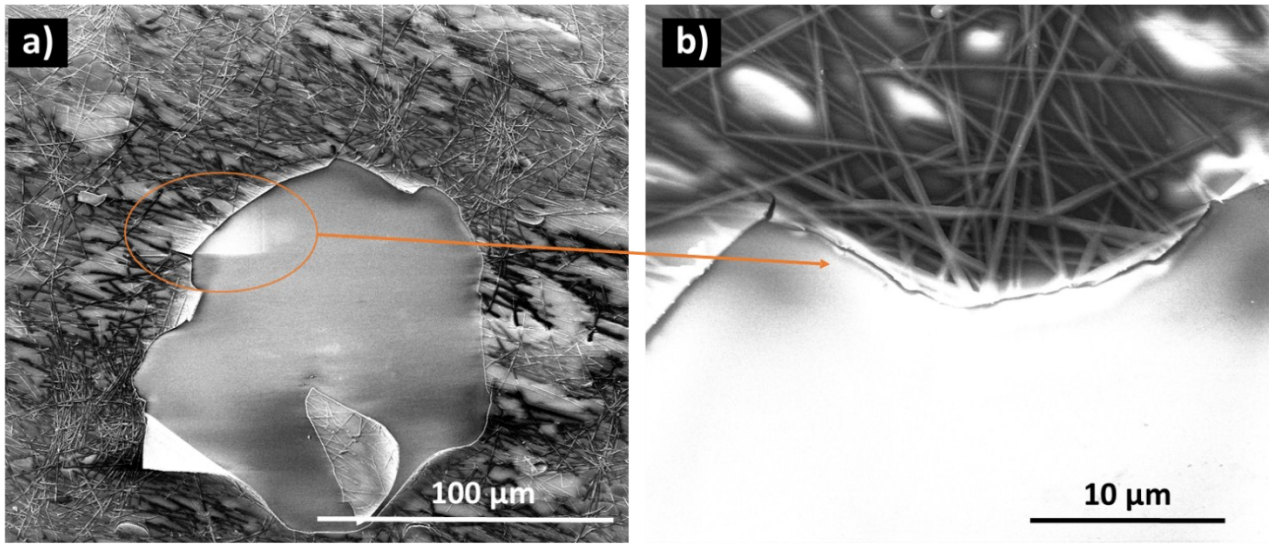

Figure SI-4. Delamination of an Al_2O_3 (80 nm) coated AgNW network deposited on corning glass observed after thermal annealing up to 400°C with a rate of 2 °C/min.

5. Thermal stability of ZnO/Al_2O_3 coated AgNW networks after 6 annealing cycles

We have observed that AgNW networks coated with bilayer coatings of ZnO/Al_2O_3, show superior thermal stability when compared to solely ZnO coated AgNW networks during identical thermal annealing process. Here, in-situ resistance measurement of bilayer coated AgNW networks during 4th and 6th cycle of thermal annealing up to 450°C is presented. No sign of irreversible change in the electrical resistance is observed.

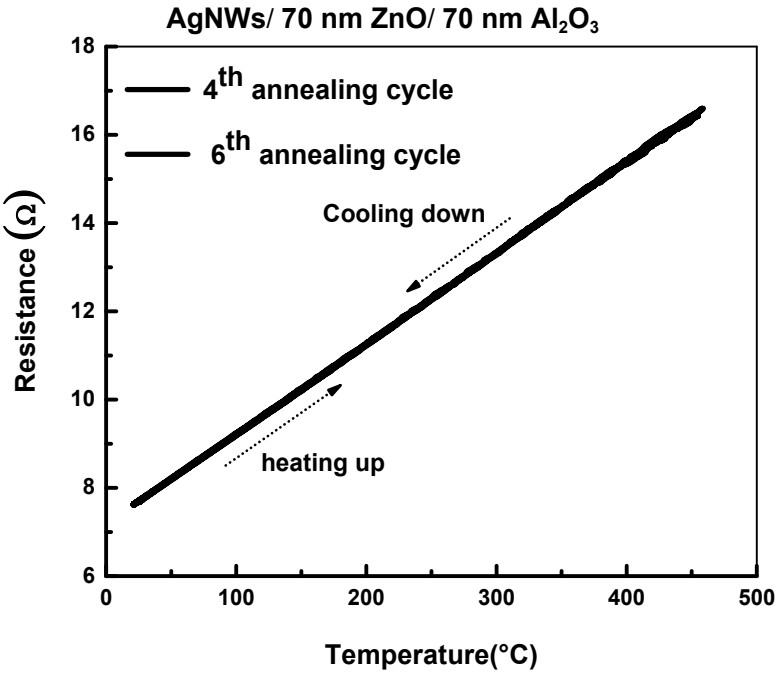

Figure SI-5 In-situ measured resistance of a AgNW network coated with 70 nm ZnO/ 70 nm Al_2O_3 bilayer during a thermal ramp up to 450 °C with a rate of 2 °C min^{-1} during fourth and sixth annealing cycles.

6. Thermal stability of bare and ZnO coated AgNW films after 10,000 bending Cycles

We have confirmed the effect of ZnO coatings on the thermal stability of AgNW networks: the thicker the ZnO film the better the network thermal stability. However, the efficiency of coatings in terms of thermal stability might be at the expense of mechanical response during bending tests. To test this potential issue we compared thermal stability during a thermal ramp up to 285°C of bare and 40 nm ZnO coated AgNW network with similar initial resistances, both after 10,000 cycles of bending (with a radius of curvature of 5 mm). The maximum temperature of annealing cycle was set at 285 °C due to the glass transition point of Neopulim substrate. Figure SI-6 clearly shows that the coated AgNW network is much more stable thermally compared to bare AgNW network, even after the 10,000 bending cycles.

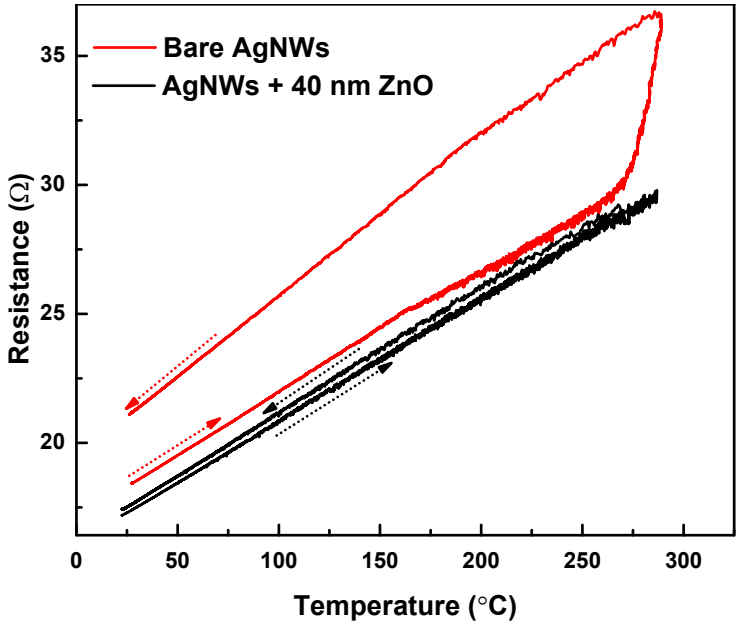

Figure SI-6. In-situ measured resistance up to 285 °C with a thermal ramp of 2 °C min^{-1} of bare AgNW network and 40 nm ZnO coated AgNW network, both after 10,000 cycles of bending (with a radius of curvature of 5 mm). The direction of the arrows show the heating up (from left to right) and cooling down (from right to left) cycles.

7. Calculation of ZnO and Al_2O_3 film thicknesses as a guide for optimizing optical transmittance of ZnO/Al_2O_3 bilayer coating on glass substrate

ZnO and Al_2O_3 have high values of bandgap energy, 3.3 eV and 8 eV, respectively. These materials have very low absorption coefficients in Vis-NIR range (380 nm–2500 nm). Therefore, as a matter of simplicity, the absorption losses in these layers have been neglected in the following calculation.

Figure SI-7 shows a schematic representation of a ZnO/Al_2O_3 bilayer coating on glass. The optimization of ZnO and Al_2O_3 film thicknesses was performed via the minimization of the light reflection from the bilayer in the visible range of 380 nm–700 nm when a normal incidence is considered. The same wavelength range was also used for calculating the experimental transmittance values as reported in Figure 2b of the manuscript.

Let us note n_0, n_1, n_2 and n_3 the refractive index of air, Al_2O_3, ZnO and glass substrate; t_1 and t_2 are the thicknesses of Al_2O_3 and ZnO layers, respectively. The light reflection from different interfaces such as air/Al_2O_3, Al_2O_3/ZnO and ZnO/glass are named r_1, r_2 and r_3, respectively. These coefficients are calculated using Fresnel's relations for normal incidence light, as follows:

$$r_1 = \frac{n_0 - n_1}{n_0 + n_1} \qquad \text{eq (1)}$$

$$r_2 = \frac{n_1 - n_2}{n_1 + n_2} \qquad \text{eq (2)}$$

$$r_3 = \frac{n_2 - n_3}{n_2 + n_3} \qquad \text{eq (3)}$$

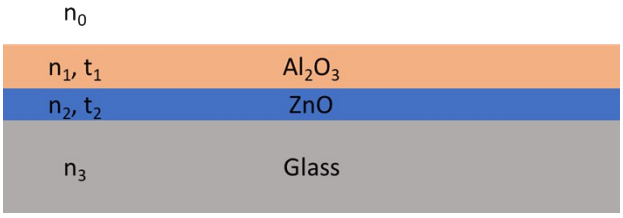

Figure SI-7. Schematic representation of a ZnO/Al_2O_3 bilayer coating on glass, in which n_0, n_1, n_2 and n_3 are the refractive index of air, Al_2O_3, ZnO and glass substrate, respectively; t_1 and t_2 are the thicknesses of Al_2O_3 and ZnO, respectively.

The phase change in each metal oxide layer can be expressed as:

$$\theta_1 = \frac{4\pi n_1 t_1}{\lambda} \qquad \text{eq (4)}$$

$$\theta_2 = \frac{4\pi n_2 t_2}{\lambda} \qquad \text{eq (5)}$$

The formula for the reflection of light *R* from a bilayer coating on glass can be written as follows:

$$R = \frac{R_A}{R_B}$$ eq (6)

Where

$$R_A = r_1^2 + r_2^2 + r_3^2 + r_1^2 r_2^2 r_3^2 + 2r_1 r_2\left(1 + r_3^2\right)\cos\theta_1 + 2r_2 r_3\left(1 + r_1^2\right)\cos\theta_2 + 2r_1$$

And

$$R_B = 1 + r_1^2 r_3^2 + r_1^2 r_2^2 + r_2^2 r_3^2 + 2r_1 r_2\left(1 + r_3^2\right)\cos\theta_1 + 2r_2 r_3\left(1 + r_1^2\right)\cos\theta_2 + 2r_1 \cos(\theta_1 - \theta_2)$$

The refractive indices n_1 and n_2 are not constant, their dependence with respect to wavelength (dispersion relation) can be found in several research articles or textbooks. In this work, we make use of the empirical equations based on the experimental data from Bond[6] for ZnO and Kumar et al.[7] for Al_2O_3, given below:

$$n_1^2 = 1.3325 + \frac{1.4068\,\lambda^2}{\lambda^2 - 0.1199}$$ eq (7)

$$n_2^2 = 2.8149 + \frac{0.8797\lambda^2}{\lambda^2 - 0.3042^2} - 0.0071\,\lambda^2$$ eq (8)

According to these dispersion relations, the refractive indices of ZnO and Al_2O_3 are represented in Figure SI-8

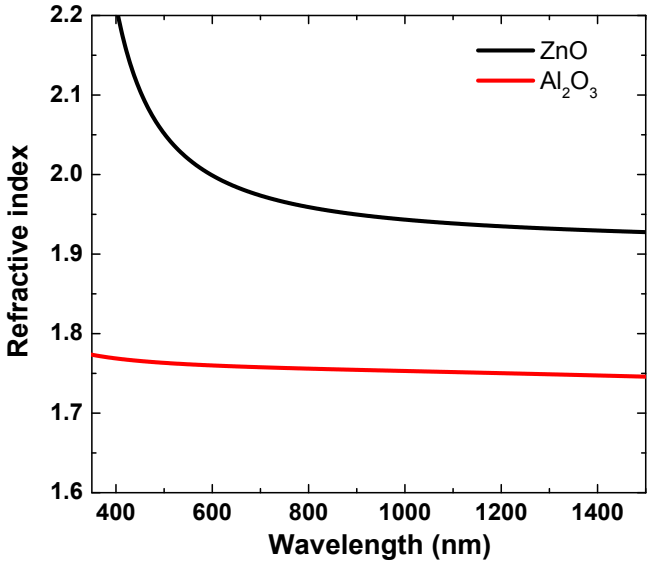

Figure SI-8. Refractive indices of ZnO and Al_2O_3 versus wavelength

By combining the dispersion relations shown in eq (7-8) and the formula calculating the reflection of ZnO/Al_2O_3 bilayer on glass shown in eq (6), the reflection of light in the visible

range of ZnO/Al_2O_3 bilayer coating on glass can be calculated versus wavelength, for a given thickness of each layer. Figure SI-9a shows the reflection in the Vis-NIR range of ZnO/ Al_2O_3 bilayer coating on glass versus wavelength for different thickness combinations of Al_2O_3 and ZnO layers. The values of the average reflection of ZnO/Al_2O_3 bilayer coating on glass calculated in the visible range (380 nm - 700 nm) as a function of coating thickness is shown in Figure SI-9b. As observed, the optimal thickness of Al_2O_3 and ZnO layers which corresponds to the minimum reflection value appears to be close to 70 nm. This was used as a guide for the experimental thickness values chosen for the experimental work reported in the manuscript.

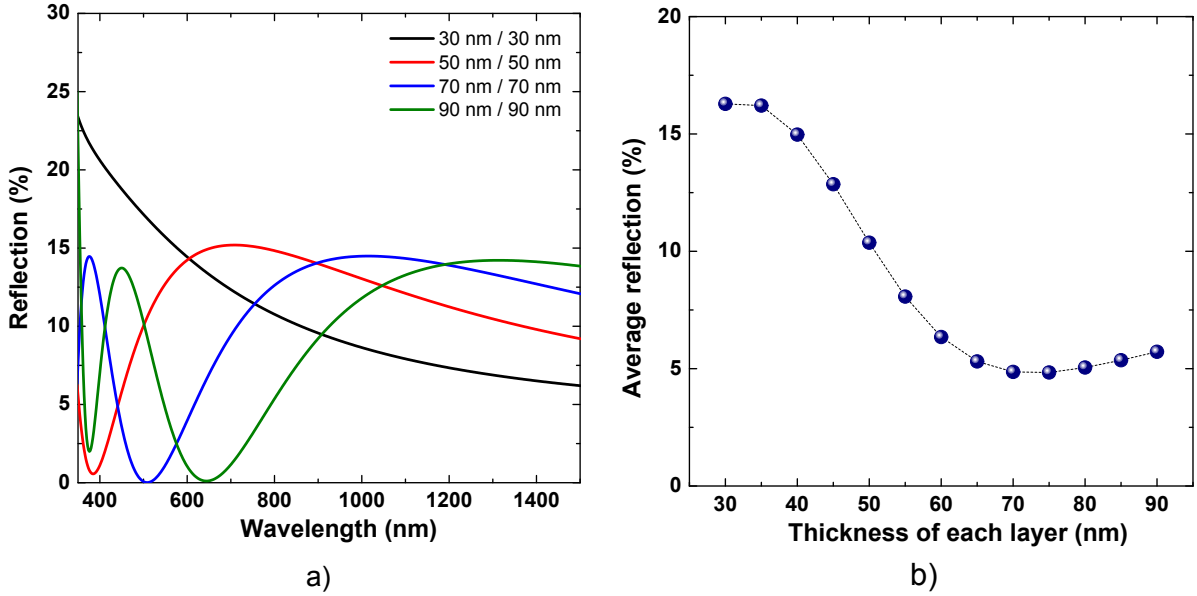

Figure SI-9. a) Optical reflection in Vis-NIR range of ZnO/Al_2O_3 bilayer coating on glass as a function of wavelength for different combinations of layer thicknesses; b) Average reflection of ZnO/Al_2O_3 bilayer coating on glass calculated in the visible range (380 nm - 700 nm) as a function of coating thickness (in this example, both Al_2O_3 and ZnO layers have a similar thickness).

Figure SI-10 shows another method of film thickness optimization, i.e. fixing the ZnO film thickness at a constant value of 70 nm while varying Al_2O_3 film thickness. Accordingly, the minimum value of the reflection of the bilayer coating on glass is close to 4.9 %, achieved at an Al_2O_3 thickness of 70 nm.

The model presented here is very simple; indeed it does not take into account the light absorption in the films nor the roughness dependence of the films on their thicknesses,[8] nor the presence of the AgNW network between the bilayer coating and the glass substrate. Nevertheless, it provides a rapid estimation of the optimum values for the coating layers. Based on these results rather similar thicknesses of the ZnO/Al_2O_3 bilayer were chosen to coat AgNW networks for the experimental proof of concept demonstrated in the manuscript.

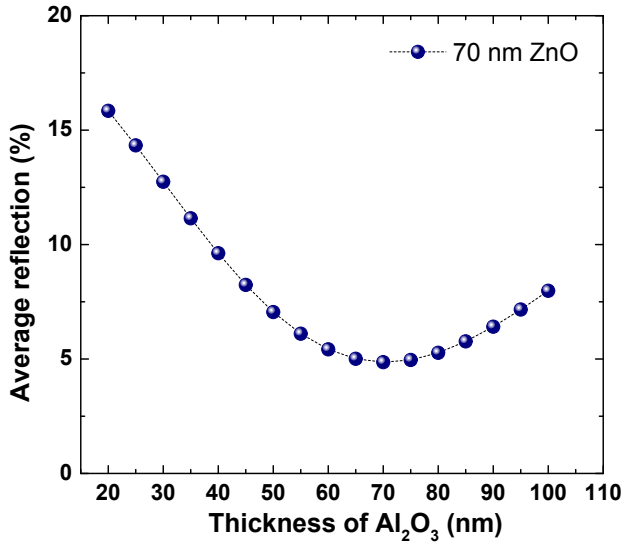

Figure SI-10. Variation of the calculated average reflection (%) in the visible range (380 nm - 700 nm) as a function of Al_2O_3 thickness when fixing ZnO thickness at 70 nm.

References:

1 D. Muñoz-Rojas and J. MacManus-Driscoll, *Mater. Horiz.*, 2014, 1, 314–320.
2 D. Muñoz-Rojas, V. H. Nguyen, C. Masse de la Huerta, S. Aghazadehchors, C. Jiménez and D. Bellet, *Comptes Rendus Phys.*, 2017, 18, 391–400.
3 V. H. Nguyen, J. Resende, C. Jiménez, J.-L. Deschanvres, P. Carroy, D. Muñoz, D. Bellet and D. Muñoz-Rojas, *J. Renew. Sustain. Energy*, 2017, 9, 021203.
4 C. Masse de la Huerta, V. H. Nguyen, J.-M. Dedulle, D. Bellet, C. Jiménez and D. Muñoz-Rojas, *Coatings*, 2019, 9, 5.
5 Q. Lin, S. Yang, W. Jing, C. Li, C. Wang, Z. Jiang and K. Jiang, *J. Electron. Mater.*, 2014, 43, 3351–3356.
6 W. L. Bond, *J. Appl. Phys.*, 1965, 36, 1674–1677.
7 P. Kumar, M. K. Wiedmann, C. H. Winter and I. Avrutsky, *Appl. Opt.*, 2009, 48, 5407.
8 V. H. Nguyen, phdthesis, Univ. Grenoble Alpes, 2018.